Integrated UAV-ALS and SLAM-TLS LiDAR for heritage tree inventory and dendrological assessment of a historical park: a case study from Jucu de Sus, Romania

Horațiu Cetean[1], Alexandra Cherecheș[2], Mircea Filipșan[1], Sergiu I. N. Mihuț[1]

[1]SC Integration Support Unit SRL, Cluj-Napoca, Romania; [2]Department of Environmental Engineering and Protection, Faculty of Agriculture, University of Agricultural Sciences and Veterinary Medicine Cluj-Napoca, Cluj-Napoca, Romania. Corresponding author: A. Cherecheș, chereches.alexandra01@gmail.com

Abstract. This study presents an integrated multi-platform LiDAR methodology for the dendrological inventory and heritage tree identification in the historical park of the Teleki-Kemény Castle estate in Jucu de Sus, Cluj County, Romania. Two complementary acquisition systems were deployed: a DJI Matrice 350 RTK equipped with the Zenmuse L2 scanner for airborne laser scanning (ALS) across the full 6.18 ha study area, and a CHCNav RS10 SLAM handheld system (hereafter referred to as the TLS acquisition component, processed via the TLS Forest module in LiDAR360) for ground-level acquisition in six representative sample plots (~500 m² each). All data were corrected through Post-Processed Kinematic (PPK) using a CHCNav I93 fixed GNSS base station and referenced in the Stereo70 coordinate system (EPSG:3844). Processing was performed in LiDAR360 v6.0 (GreenValley International). After geometric alignment and a six-class point cloud classification combining progressive TIN filtering, Cloth Simulation Filter (CSF), Deep Learning-assisted segmentation, and manual refinement, a total of 1,890 individual trees and shrubs were identified across the site. Six representative sample plots were processed using the TLS Forest segmentation algorithm (LiDAR360), yielding individual-level dendrometric measurements — total height (H), trunk diameter at 1.3 m (DBH), and crown diameter (Dc) — for 351 individuals. Thirty remarkable trees were georeferenced within the sample plots, and 37 additional heritage-candidate trees were mapped at site level, totalling 67 heritage candidates. The most structurally significant individual recorded attained H = 24.6 m, DBH = 94.1 cm, and Dc = 17.7 m. Complementary floristic analysis (three Braun-Blanquet relevés, 100 m² each) identified the vegetation as belonging to the association Symphyto officinalis–Anthriscetum sylvestris Passarge 1975, with Fraxinus excelsior and Acer campestre as dominant arboreal species. The integrated ALS–TLS workflow proved effective for precise digital inventory at the individual tree level, supporting conservation planning, structural risk assessment, and long-term monitoring of a historically significant urban park.
Keywords: airborne laser scanning, SLAM, terrestrial LiDAR (TLS module), individual tree segmentation, heritage dendrology, point cloud classification, urban park inventory, LiDAR360, Stereo70.

Introduction. Accurate inventorying of urban and peri-urban trees constitutes a fundamental prerequisite for both ecological management and the preservation of heritage landscapes. In the context of historically significant parks associated with noble estates, this challenge is compounded by the need to document not only tree dimensions and spatial positions, but also the cultural and structural legacy encoded in centuries-old individuals. Classical dendrometric methods, while rigorous at the plot level, are inherently limited by sampling effort, measurement uncertainty at height, and the practical impossibility of achieving complete spatial coverage across complex terrain (Moskal et al., 2009).

Light Detection and Ranging (LiDAR) technology has progressively established itself as the most capable remote sensing tool for three-dimensional forest characterisation. Airborne laser scanning (ALS) enables rapid, high-density data acquisition across large areas, providing reliable canopy height models and individual tree detection through crown-based segmentation algorithms (Donoghue et al., 2007; Kaartinen et al., 2012; Cosenza et al., 2022). Individual tree segmentation from ALS data relies on detecting local maxima as crown apices and delineating tree crowns through graph-cut or region-growing approaches (Li et al., 2012; Dalponte & Coomes, 2016). Mobile terrestrial laser scanning, particularly systems employing Simultaneous Localisation and Mapping (SLAM) algorithms, complements ALS data by capturing sub-canopy structure, trunk geometry, and ground-level detail inaccessible from aerial platforms (Liang et al., 2016; Hyyppä et al., 2020).

The fusion of multi-platform LiDAR data — aerial and terrestrial — offers a comprehensive reconstruction of individual tree morphology, including total height, diameter at breast height (DBH), and crown dimensions, parameters central to dendrological assessment and structural risk evaluation (Moskal et al., 2009; Calders et al., 2015; Cosenza et al., 2022). While these approaches have been extensively validated in plantation and managed forest contexts, their application to historical urban parks with complex mixed vegetation and significant anthropogenic influence remains insufficiently explored.

The study site, located in Jucu de Sus (Cluj County, Romania) and associated with the former Teleki-Kemény noble estate (LMI code CJ-II-m-B 07686), presents particular challenges and opportunities. The 6.18 ha area encompasses a mosaic of mature heritage trees, spontaneous woody regeneration, invasive species stands, and geomorphologically complex terrain. Historical evidence and photographic records indicate the past existence of structured garden layouts, mill canal alignments, and tree avenues, of which certain individuals may persist as living heritage witnesses.

The objective of this study was to develop and apply an integrated ALS–TLS workflow for: (i) complete site-level individual tree detection and spatial mapping across the 6.18 ha area; (ii) precise dendrometric characterisation of trees in six representative sample plots using TLS-based segmentation; (iii) identification and georeferencing of heritage-candidate trees based on structural and dimensional criteria; and (iv) floristic characterisation of the vegetation community through phytosociological analysis.

Material and Method

Description of the study site*.* The study area is located in the village of Jucu de Sus, Jucu commune, Cluj County, Romania, at the base of the promontory occupied by the Teleki-Kemény Castle (centroid coordinates approximately 46°51'N, 23°52'E; Stereo70: X ≈ 407,950; Y ≈ 596,210). The total area of the analysed site was (61,787 m²). The terrain transitions from a steep northwest-facing slope (inclination approximately 45–50%) adjacent to the castle promontory to the floodplain of the Someșul Mic river.

All spatial data produced in this study were referenced to the Stereo70 coordinate system (Pulkovo 1942(58) / Stereo70, EPSG:3844). The aerial orthomosaic providing the 2D base layer is presented in Figure 1.

Data acquisition equipment*.* Three complementary systems were deployed, covering the complete geospatial data collection chain:

DJI Matrice 350 RTK + DJI Zenmuse L2. Multirotor UAV with integrated LiDAR scanner (905 nm; FOV 70°; up to 5 returns per pulse; range accuracy ≤ 4 cm; maximum pulse repetition rate 240 kHz) and RGB camera; used for ALS acquisition and photogrammetric orthomosaic generation.

CHCNav RS10 SLAM System. Handheld SLAM 3D laser scanner integrating GNSS RTK and visual SLAM (32 channels; range 300 m; FOV 210° × 170°; absolute accuracy < 5 cm H/V; relative accuracy < 1 cm); deployed for ground-level acquisition in areas of dense vegetation or restricted UAV access.

CHCNav I93 GNSS Base Station. Fixed RTK/PPK reference receiver providing correction data for geometric co-registration of all datasets in Stereo70.

Figure 1. Aerial RGB orthomosaic of the study area (total extent 6.18 ha; GSD = 2.12 cm/pixel; DJI Matrice 350 RTK / Zenmuse L2). The Teleki-Kemény Castle promontory is visible in the upper left portion of the image. Coordinate system: Stereo70 (EPSG:3844).
Map source: Nations online 2016.

Aerial data acquisition. Two distinct UAV flight missions were executed over the 6.18 ha study area. The LiDAR ALS mission was conducted at 70 m AGL, achieving a mean point density of approximately 300 pts m^{-2} over the full site, with a 60% lateral strip overlap. The photogrammetric mission was conducted at 50–60 m AGL, yielding 304 images processed in DJI Terra via the PPK method; the resulting orthomosaic achieved GSD = 2.12 cm/pixel. Both datasets were PPK-corrected using the CHCNav I93 base station, ensuring planimetric and altimetric accuracy at centimetre level.

Point cloud processing workflow. All point cloud processing was performed in LiDAR360 v7.0 (GreenValley International, 2022).

Geometric alignment and fusion. The ALS (.LAS, Zenmuse L2) and SLAM-acquired terrestrial (.LAS, CHCNav RS10) point cloud datasets were independently acquired and subsequently fused after geometric alignment verified on the X, Y, and Z axes through comparative surface analysis. Co-registration quality was checked by comparing overlapping stable surface features on the X, Y, and Z axes prior to merging.

Point cloud classification. The unified point cloud was subjected to a four-stage automatic classification pipeline: (1) Low Point Classification — removal of sub-ground anomalous points; (2) CSF (Cloth Simulation Filter; Zhang et al., 2016) — ground point extraction through flexible surface simulation; (3) Median Filter — soil classification refinement; (4) Height Normalisation — Z-value correction relative to the interpolated DTM. Final classification employed progressive TIN filtering, Deep Learning-based detection, and manual interactive editing, yielding six classes: ground, low vegetation, high vegetation, buildings, and infrastructure (Figure 2).

Individual tree segmentation — ALS. Individual tree segmentation from the normalised ALS point cloud used an automated crown-based algorithm (ALS Cloud Segmentation module, LiDAR360), following the approach of Li et al. (2012), identifying local maxima as tree apex positions and assigning a unique Tree ID to each point cluster. The initial automatic segmentation identified 2,189 individuals. Systematic manual review removed misclassified anthropogenic elements (buildings, vehicles, power lines), yielding a final inventory of 1,890 individuals (Figure 3).

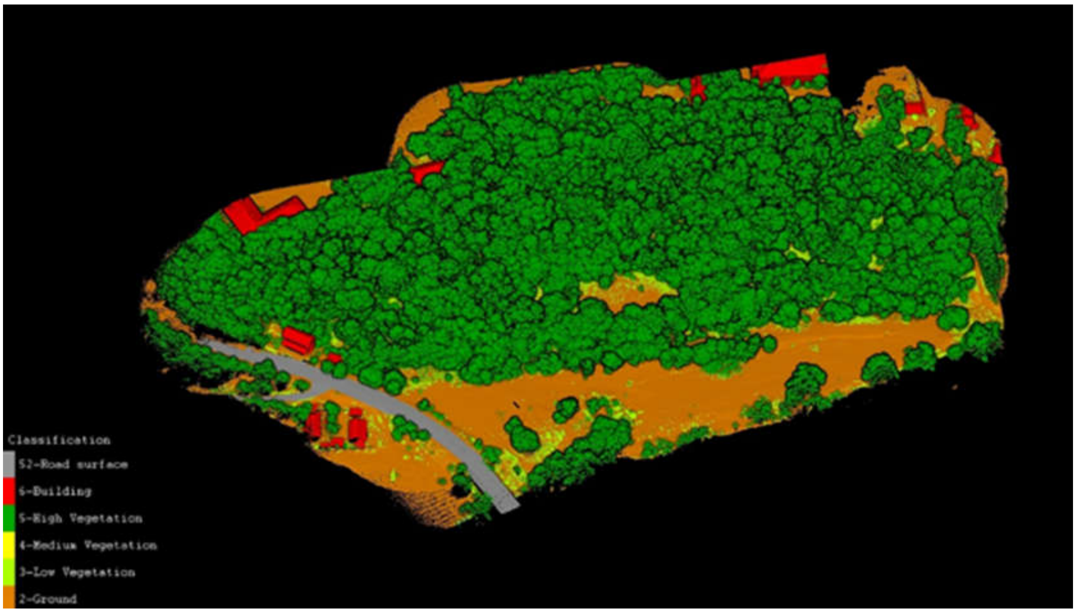

Figure 2. Final six-class point cloud classification of the unified ALS–TLS dataset. Classes: ground points (brown), low vegetation (light green), high vegetation (dark green), buildings (red), infrastructure (grey), Classification combined progressive TIN filtering, CSF, Deep Learning automation, and manual refinement.

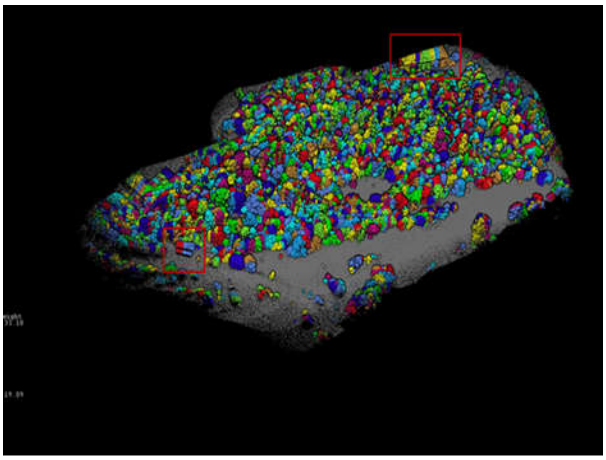

(a) Initial ALS segmentation — 2,189 individuals

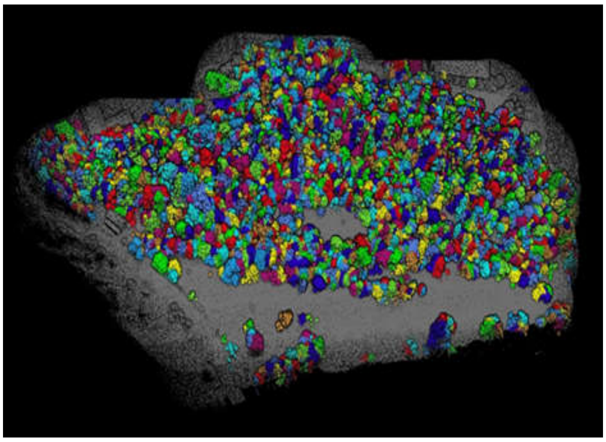

(b) Final segmentation after manual refinement — 1,890 individuals

Figure 3. ALS-based individual tree segmentation: (a) initial automatic result including misclassified anthropogenic objects; (b) final dataset after manual reclassification across the 6.18 ha study area.

Individual tree segmentation — TLS (SLAM-Acquired Data). Six representative sample plots (~500 m² each) were processed using the TLS Forest module (LiDAR360), providing trunk-level measurements of H, DBH, and Dc for 351 individuals through a bottom-up segmentation algorithm that captures trunk geometry not accessible from ALS (Liang et al., 2016). The six plot centroids and individual counts are given in Table 1; their spatial distribution is shown in Figure 4.

Table 1

Location and characteristics of the six TLS sample plots
(data acquired via CHCNav RS10 SLAM) (Stereo70 coordinate system, EPSG:3844)

Plot	*X (Stereo70)*	*Y (Stereo70)*	*Area (m²)*	*N individuals*
1	407,942.988	596,145.028	~500	93
2	407,972.370	596,165.590	~500	58
3	407,951.377	596,197.338	~500	39
4	407,946.369	596,242.422	~500	51
5	407,911.380	596,271.274	~500	40
6	407,930.313	596,298.712	~500	70
Total	—	—	~3,000	351

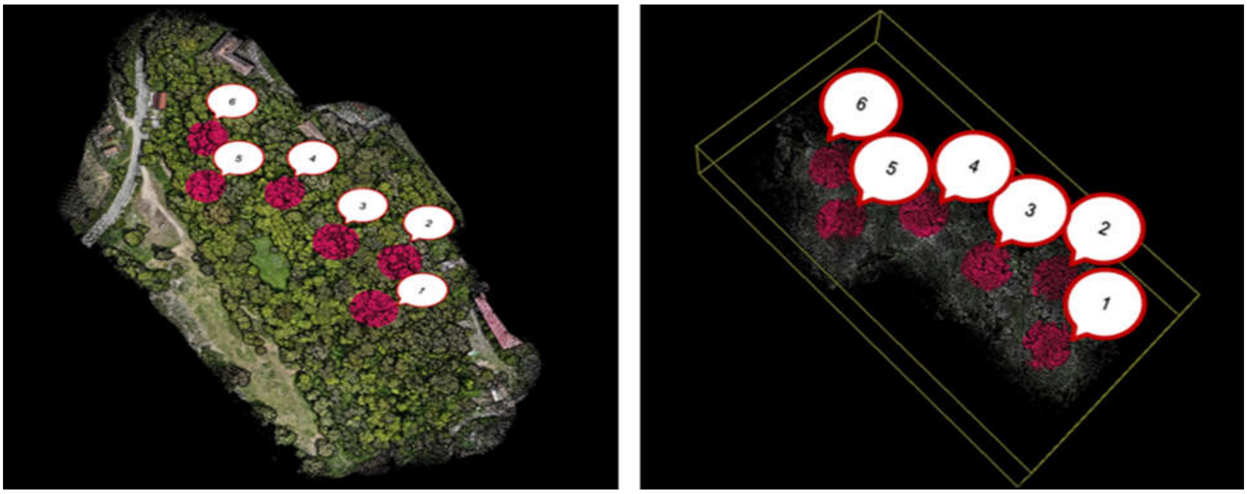

Figure 4. Spatial distribution of the six TLS sample plots (acquired via CHCNav RS10 SLAM) (~500 m² each) across the study area, superimposed on the point cloud RGB base. Each plot was processed independently using the TLS Forest segmentation algorithm (LiDAR360).

Floristic analysis*.* Three phytosociological relevés (100 m² each) were conducted following the Braun-Blanquet method (Braun-Blanquet, 1964), with cover-abundance estimated using the standard scale (r, +, 1–5). Vegetation was stratified into arboreal (A), shrub (S), and herbaceous (H) layers. Ecological characterisation used Ellenberg indicator values (Ellenberg et al., 1992) for light (L), temperature (T), moisture (F), soil reaction (R), nitrogen (N), and continentality (K). Community-weighted Ellenberg indicator values were calculated from Braun-Blanquet cover-abundance data using the LiANA web-based software platform (Integration Support Unit SRL, 2001), based on Ellenberg indicator values following Ellenberg et al. (1992).

Trees were designated as heritage candidates upon meeting at least two of the following criteria: (i) H > 20 m; (ii) DBH > 50 cm; (iii) Dc > 10 m; or (iv) spatial position consistent with historical landscape elements of the Teleki-Kemény estate documented in historical records. All candidate trees were georeferenced in Stereo70. Species identification was performed by field observation during TLS scanning campaigns.

Results and Discussion

Point cloud acquisition and classification*.* The integrated LiDAR acquisition yielded two complementary datasets: an ALS dataset covering the full 6.18 ha at ~300 pts m^{-2}, and six TLS subplot datasets (acquired with CHCNav RS10 SLAM) for ground-level structural characterisation. The unified point cloud in Stereo70 provided the basis for all subsequent processing. The six-class final classification provided reliable vegetation-to-infrastructure separation, enabling individual tree segmentation. Secondary cartographic products derived from the LiDAR-classified ground surface include a Digital Elevation Model (DEM) (Figure 5).

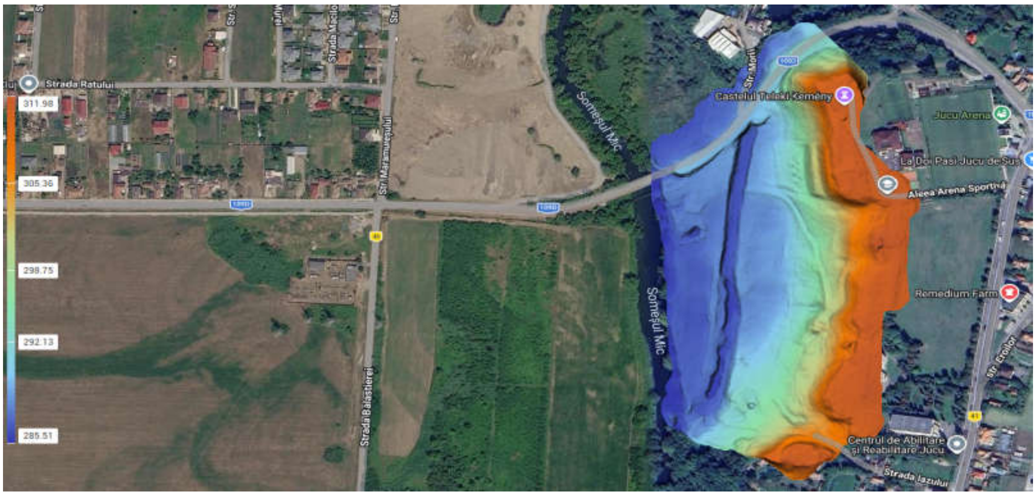

Figure 5. Digital Elevation Model (DEM) of the study area derived from the LiDAR ground point classification (LiDAR360). The morphological transition from the castle promontory slope (northwest) to the Someșul Mic floodplain (east) is clearly.

Individual tree detection — site level. ALS-based segmentation after manual refinement yielded 1,890 individual trees and shrubs across the 6.18 ha site (~306 individuals ha^{-1}). Thirty trees within the six sample plots and 37 additional trees at site level were georeferenced as heritage-candidate individuals (67 total). Their spatial distribution is shown in Figure 6.

Figure 6. Spatial distribution of heritage-candidate trees (elements of interest with high dendrometric values or historical significance) across the 6.18 ha site, overlaid on the ALS-derived RGB point cloud. Each marker represents an individual meeting at least two heritage designation criteria.

Dendrometric characteristics of sample plots. The 351 individuals across the six plots showed marked structural variability. Plot 1 had the highest individual count (93), reflecting dense slope regeneration. Plots 5 and 6 — situated in the transitional and floodplain sectors respectively — exhibited the greatest individual-level dimensions, consistent with mature trees of probable historical origin. Figure 7 shows 3D representations of Plots 5 and 6, those containing the most prominent heritage candidates.

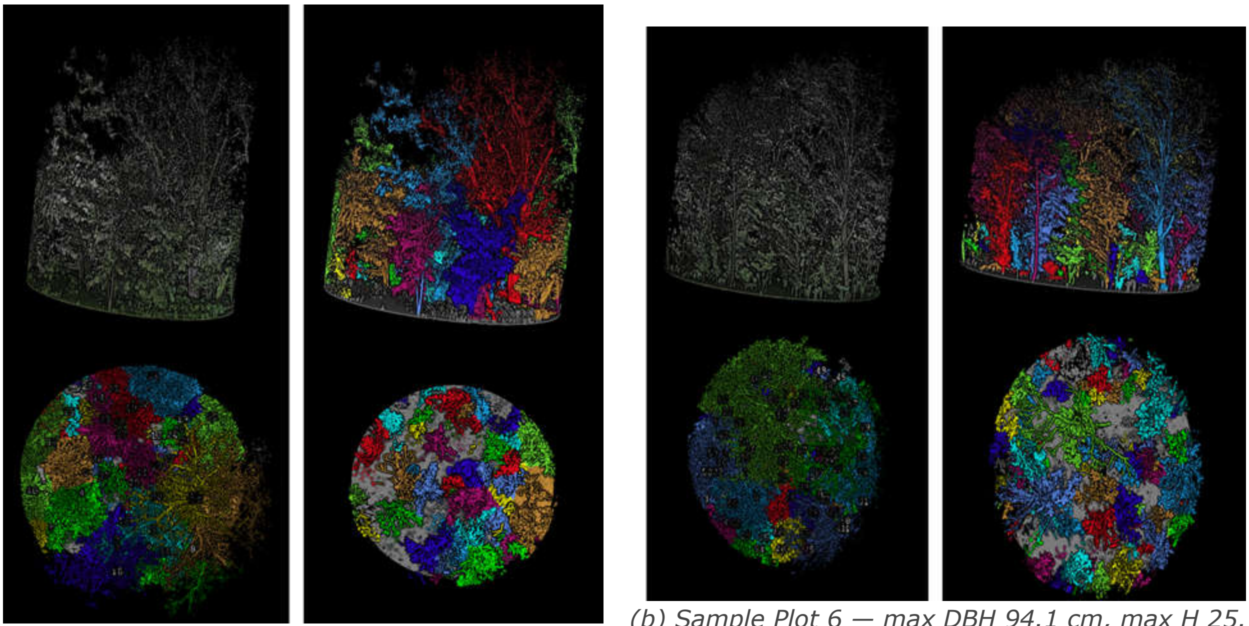

(a) Sample Plot 5 — max DBH 91.2 cm, max H 26.0 m

(b) Sample Plot 6 — max DBH 94.1 cm, max H 25.7 m

Figure 7. TLS-derived 3D point cloud (RGB) representations of Sample Plots 5 (a) and 6 (b), containing the most structurally prominent heritage-candidate individuals. Individual tree segmentation (TLS Forest module (LiDAR360) is shown with unique colour per Tree ID.

Table 2

Selected heritage-candidate trees from TLS-derived dendrometric attributes (LiDAR360 TLS Forest module; data acquired via CHCNav RS10 SLAM)

Plot	*Tree ID*	*Species*	*H (m)*	*DBH (cm)*	*Dc (m)*	*X (Stereo70)*	*Y (Stereo70)*
1	61	*Fraxinus excelsior*	22.6	74.3	17.5	407.939.3	596.141.5
4	49	*Fraxinus excelsior*	28.2	55.8	10.4	407.956.0	596.240.3
5	23	*Fraxinus excelsior*	25.4	91.2	12.9	407.960.5	596.165.4
5	12	*Fraxinus excelsior*	26.0	85.7	12.6	407.975.5	596.162.8
6	70	***Populus nigra***	**24.6**	**94.1**	**17.7**	**407.930.3**	**596.304.5**
6	14	*Fraxinus excelsior*	25.7	47.7	14.0	407.941.8	596.298.2
6	6	*Acer campestre*	19.6	42.2	8.9	407.925.9	596.294.8

Notes: Species determined by field observation during scanning campaigns. Coordinates in Stereo70 (EPSG:3844). H = total height; DBH = trunk diameter at 1.3 m; Dc = crown diameter. Bold row: most structurally prominent individual.

Plot 6, Tree 14 (DBH = 47.7 cm, Dc = 14.0 m) and Plot 6, Tree 6 (H = 19.6 m, Dc = 8.9 m) are included on the basis of criterion (iv) — spatial position at the historical floodplain plantation alignment — in combination with one morphological criterion each.

Floristic analysis and vegetation structure. The three relevés (total cover 85–95%) were assigned to the association *Symphyto officinalis–Anthriscetum sylvestris* Passarge 1975, assigned to the alliance *Aegopodion podagrariae* Tx. 1967, order *Galio-Alliarietalia* Oberd. in Görs et T. Müller 1969, and class *Galio-Urticetea* Passarge ex Kopecký 1969 (Sanda, 2002). The arboreal layer was dominated by *Fraxinus excelsior* and *Acer campestre* (Relevés 1–2) and *Aesculus hippocastanum* (Relevé 3). The invasive neophyte *Acer negundo* occurred in Relevés 1 and 3; *Sambucus nigra* dominated the shrub layer consistently. Figure 8 shows field perspectives from Relevé 1.

Figure 8. Vegetation structure in Sample Relevé 1 (northwest-facing slope, inclination ~46%). Dominant Acer negundo in the arboreal layer (background) with dense Aegopodium podagraria herbaceous cover (foreground). Overall cover ~85%; Ellenberg moisture (F) and nitrogen (N) values elevated.

Table 3

Simplified synoptic Braun-Blanquet cover-abundance table

Species	*Layer*	*Relevé 1*	*Relevé 2*	*Relevé 3*
Fraxinus excelsior	A	2	3	2
Acer campestre	A/S	—	2	1
*Acer negundo**	A/S	3	—	1
Aesculus hippocastanum	A	—	—	3
Sambucus nigra	S	2	2	1
Aegopodium podagraria	H	5	3	—
Ranunculus ficaria	H	4	4	4
Galium aparine	H	2	5	3
Urtica dioica	H	1	4	3
Anthriscus sylvestris	H	+	2	3
Symphytum officinale	H	—	—	2
Lamium purpureum	H	1	1	2

A = arboreal; S = shrub; H = herbaceous layer; * = invasive alien species; — = absent.

The elevated N values (7.3–7.9) across all three relevés confirm anthropogenic nitrogen enrichment, consistent with the site's proximity to agricultural and ruderal inputs. Elevated F values (6.1–6.8) reflect the hydrological influence of the Someșul Mic floodplain and the northwest-facing slope regime. Low L values (4.6–4.9) indicate strong canopy closure. These patterns collectively characterise the site as a mesophilous-to-hygrophilous eutrophic ecotone, typical of the *Aegopodion podagrariae* alliance (Mucina et al., 2016).

Table 4

Community-weighted mean Ellenberg indicator values per relevé, computed via LiANA software; Ellenberg indicator values after Ellenberg et al. (1992)

Relevé / Indicator	*L*	*T*	*F*	*R*	*N*	*K*
Relevé 1	4.9	5.4	6.2	7.1	7.8	3.2
Relevé 2	4.6	5.3	6.1	7.0	7.9	3.1
Relevé 3	4.7	5.4	6.8	7.2	7.3	3.3
Ecological interpretation	Semi-shade	Temperate	Moist–hygrophilous	Neutral–alkaline	Eutrophic	Sub-oceanic

L = light; T = temperature; F = moisture; R = soil reaction; N = nitrogen; K = continentality.

The vegetation mosaic across the site comprised four main units: dense nitrophilous herbaceous vegetation (80–95% cover; Figure 9a), zones of woody regeneration (*Fraxinus excelsior/Acer campestre* dominance), anthropically influenced ruderal sectors (*Acer negundo, Gleditsia triacanthos*), and the structurally dominant large-tree zone in the floodplain sector (*Populus nigra, Platanus* × *hispanica*; Figure 9b).

(a) Dense nitrophilous herbaceous vegetation (Urtica / Galium aparine)

(b) Large-diameter trees in the Someșul Mic floodplain

Figure 9. Characteristic vegetation units of the study area: (a) dense nitrophilous herbaceous cover dominated by *Urtica dioica* and *Galium aparine*, typical of the *Symphyto officinalis–Anthriscetum sylvestris* association; (b) large-diameter *Populus nigra* and *Platanus* × *hispanica* individuals in the floodplain sector with structural and heritage significance.

Avifaunistic and faunistic observations. Opportunistic faunistic observations were conducted simultaneously with field campaigns (April–May 2024, with a total observation effort of approximately 12 person-hours across three site visits). Thirteen bird species were recorded: *Sylvia atricapilla, Fringilla coelebs, Luscinia megarhynchos, Parus major, Buteo buteo, Passer domesticus, Corvus corax, Coloeus monedula, Oriolus oriolus, Sturnus vulgaris, Cyanistes caeruleus, Turdus merula*, and *Streptopelia decaocto*. The assemblage is dominated by common woodland-edge and generalist species; no Annex I species under Directive 2009/147/EC were confirmed. *Capreolus capreolus* was also recorded on multiple occasions at the forest-floodplain interface, indicating maintenance of functional habitat connectivity between the riparian corridor and the adjacent semi-natural areas. These observations are reported as qualitative context for the site's ecological value and do not constitute a systematic faunistic survey.

ALS–TLS integration for heritage tree identification. The integrated multi-platform LiDAR approach demonstrated its effectiveness for complete, spatially explicit dendrological inventorying in a historically complex urban park. The ALS platform provided site-wide coverage and enabled census-level individual detection (1,890 individuals across 6.18 ha), consistent with the area-based approach used in plantation forestry studies (Donoghue et al., 2007; Kaartinen et al., 2012; Cosenza et al., 2022). The complementary TLS dataset (acquired via CHCNav RS10 SLAM, processed through the TLS Forest module in LiDAR360) provided sub-canopy structural detail and direct trunk-level measurement, enabling DBH estimation critical for heritage tree assessment — a parameter ALS alone cannot reliably extract due to crown occlusion of the trunk (Moskal et al., 2009; Liang et al., 2016).

The combined approach addresses a core limitation of single-platform studies. ALS-derived metrics excel in characterising canopy height and crown geometry but systematically underestimate DBH in complex mixed-species stands (Donoghue et al., 2007; Calders et al., 2015). TLS-derived DBH values reaching 94.1 cm (Plot 6, Tree 70) cannot be reliably extracted from ALS data alone, yet represent the most critical parameter for heritage classification. PPK correction with the CHCNav I93 base station ensured positional consistency in the Stereo70 frame, enabling long-term spatial repeatability for future monitoring campaigns.

Heritage tree candidates and historical landscape context. The most structurally prominent individuals — concentrated in sample Plots 5 and 6 in the northern sector — exhibit dendrometric characteristics consistent with mature specimens potentially associated with the historical Teleki-Kemény estate landscape layout. Plot 5 Trees 12 (H = 26.0 m, DBH = 85.7 cm, *Fraxinus excelsior*) and 23 (H = 25.4 m, DBH = 91.2 cm, *Fraxinus excelsior*), and Plot 6 Tree 70 (H = 24.6 m, DBH = 94.1 cm, Dc = 17.7 m, *Populus nigra*) constitute the prime heritage candidates on morphological grounds. Their spatial distribution is consistent with the historical mill canal system and slope-edge plantation patterns documented in estate records, although definitive attribution of biological age would require dendrochronological analysis beyond the scope of this study.
The LiDAR-derived DEM confirmed the persistence of a morphological depression corresponding to the former mill canal route — a morphological feature spatially consistent with the former mill canal route, providing independent spatial corroboration for historical landscape reconstruction. This integration of 3D terrain modelling with vegetation inventory represents a methodological advance in historical park characterisation, consistent with the precision forestry approach advocated by Moskal et al. (2009).

Vegetation structure and ecological implications. The *Symphyto officinalis–Anthriscetum sylvestris* association reflects the nitrophilous ecotonal character of the site, consistent with its position between the castle slope and the riparian corridor. Community-weighted Ellenberg N values (7.3–7.9) indicate strong anthropogenic nitrogen enrichment across all three relevés. The recurrent presence of the invasive neophyte *Acer negundo* within the arboreal layer of two of the three relevés suggests ongoing anthropogenic disturbance and secondary vegetation dynamics (Sîrbu et al., 2011).

Monitoring framework. The generated dataset constitutes the baseline for a long-term monitoring protocol: (i) annual multispectral surveys for Normalized Difference Vegetation Index (NDVI)-based vitality assessment of heritage trees; (ii) periodic LiDAR re-acquisition (3–5-year intervals, or following extreme meteorological events) for structural change detection at the individual tree level. This framework follows the principle of predictive, non-destructive monitoring advocated by Cosenza et al. (2022), adapted here to heritage conservation objectives. The precise georeferencing of all 67 heritage-candidate trees in Stereo70 provides the spatial anchor for all future monitoring campaigns.

Conclusions. This study demonstrated that the integration of UAV-ALS and SLAM-based terrestrial LiDAR (processed via the TLS module in LiDAR360) provides a robust, spatially complete methodology for dendrological inventory and heritage tree identification in historically complex urban parks. Applied to the 6.18 ha Teleki-Kemény estate park in Jucu de Sus, Romania, the workflow yielded a site-level inventory of 1,890 trees and shrubs, detailed dendrometric characterisation of 351 individuals across six sample plots, and georeferenced identification of 67 heritage-candidate trees in the Stereo70 reference system.

The most structurally significant individuals — including *Fraxinus excelsior* specimens with DBH exceeding 85 cm and a *Populus nigra* individual attaining DBH = 94.1 cm and crown diameter of 17.7 m — are spatially consistent with the historical layout of the Teleki-Kemény estate and represent irreplaceable ecological and cultural assets requiring dedicated conservation measures. Their spatial positions are furthermore corroborated by the LiDAR-derived DEM, which confirms the morphological trace of the former estate mill canal.

The complementarity of ALS and TLS data proved essential: ALS enabled rapid, site-wide crown-level detection while the SLAM-acquired TLS data provided trunk measurements critical for heritage classification. Floristic analysis identified the *Symphyto officinalis–Anthriscetum sylvestris* association, with elevated nitrogen values (Ellenberg N 7.3–7.9) and presence of invasive alien species (*Acer negundo, Gleditsia triacanthos*) requiring active management.

The resulting digital inventory — precisely classified point cloud, individual tree GPS coordinates in Stereo70, dendrometric attribute database, community-weighted Ellenberg indices, phytosociological characterisation — constitutes the technical foundation for the park management plan, structural risk assessment, and a repeatable long-term LiDAR monitoring protocol.

Authors Contributions. HC and AC wrote the manuscript; SINM and MF read and revised the manuscript.

Conflicts of Interest. The authors declare that there is no conflict of interest.

Data Availability. The data supporting the findings of this study are available from the corresponding author upon reasonable request.

Funding. This research received no external funding.

References

Braun-Blanquet, J. (1964). *Pflanzensoziologie: Grundzüge der Vegetationskunde* (3rd ed.). Springer, Wien.

Calders, K., Newnham, G., Burt, A., Murphy, S., Raumonen, P., Herold, M., et al. (2015). Nondestructive estimates of above-ground biomass using terrestrial laser scanning. *Methods in Ecology and Evolution, 6*(2), 198–208.

Cosenza, D.N., Vogel, J., Broadbent, E.N., & Silva, C.A. (2022). Silvicultural experiment assessment using lidar data collected from an unmanned aerial vehicle. *Forest Ecology and Management, 522*, 120489.

Dalponte, M., & Coomes, D.A. (2016). Tree-centric mapping of forest carbon density from airborne laser scanning and hyperspectral data. *Methods in Ecology and Evolution, 7*(10), 1236–1245.

Donoghue, D.N.M., Watt, P.J., Cox, N.J., & Wilson, J. (2007). Remote sensing of species mixtures in conifer plantations using LiDAR height and intensity data. *Remote Sensing of Environment, 110*(4), 509–522.

Ellenberg, H., Weber, H.E., Düll, R., Wirth, V., Werner, W., & Paulissen, D. (1992). Zeigerwerte von Pflanzen in Mitteleuropa. *Scripta Geobotanica, 18*, 1–258.

European Parliament & Council of the European Union. (2009, November 30). *Directive 2009/147/EC on the conservation of wild birds (Codified version).* Official Journal of the European Union, L 20, 7–25.

GreenValley International. (2022). LiDAR360 (Version 6.0) [Software]. GreenValley International Ltd. https://greenvalleyintl.com/software/lidar360/

Hyyppä, E., Hyyppä, J., Hakala, T., Kukko, A., Wulder, M.A., White, J.C., et al. (2020). Under-canopy UAV laser scanning for accurate forest field measurements. *ISPRS Journal of Photogrammetry and Remote Sensing, 164*, 41–60.

Kaartinen, H., Hyyppä, J., Yu, X., Vastaranta, M., Hyyppä, H., Kukko, A., et al. (2012). An international comparison of individual tree detection and extraction using airborne laser scanning. *Remote Sensing, 4*(4), 950–974.

Li, W., Guo, Q., Jakubowski, M.K., & Kelly, M. (2012). A new method for segmenting individual trees from the LiDAR point cloud. *Photogrammetric Engineering & Remote Sensing, 78*(1), 75–84.
Liang, X., Kankare, V., Hyyppä, J., Wang, Y., Kukko, A., Haggrén, H., … Vastaranta, M. (2016). Terrestrial laser scanning in forest inventories. *ISPRS Journal of Photogrammetry and Remote Sensing, 115*, 63–77.
Moskal, L.M., Erdody, T., Kato, A., Richardson, J., Zheng, G., & Briggs, D. (2009). Lidar applications in precision forestry. *Proceedings of the ISPRS Workshop on Laser Scanning 2009*, Paris.
Mucina, L., Bültmann, H., Dierßen, K., Theurillat, J.-P., Raus, T., Čarni, A., et al. (2016). Vegetation of Europe: Hierarchical floristic classification system of vascular plant, bryophyte, lichen, and algal communities. *Applied Vegetation Science, 19*(Suppl. 1), 3–264.
Sanda, V. (2002). *Ceno-structural Vademecum on the Vegetation Cover of Romania*. Vergili, Bucharest. [In Romanian]
Sîrbu, C., & Oprea, A. (2011). Invasive plants in Romania. "Ion Ionescu de la Brad" University Press, Iași. [In Romanian]
Zhang, W., Qi, J., Wan, P., Wang, H., Xie, D., Wang, X., & Yan, G. (2016). An easy-to-use airborne LiDAR data filtering method based on cloth simulation. *Remote Sensing, 8*(6), 501.
*** Integration Support Unit SRL. (2001). *LiANA: Web-based software platform for floristic data processing and Ellenberg indicator calculation* liana.bio. Available online: liana.bio [Last view: June 2026]

Received: 12 May 2026. Accepted: 17.06.2026. Published online: 18.06.2026.
Authors:
Horațiu Cetean (HC), SC Integration Support Unit SRL, 35 Baladei Street, 400372 Cluj-Napoca, Romania, e-mail: horatiu.cetean@gmail.com
Alexandra Chereches (AC), University of Agricultural Sciencesand Veterinary Medicine Cluj-Napoca, Faculty of Agriculture, 3-5 Mănăștur Street, 400372 Cluj-Napoca, Romania, e-mail: chereches.alexandra01@gmail.com
Mircea Filipșan (MF), SC Integration Support Unit SRL, 35 Baladei Street, 400372 Cluj-Napoca, Romania, e-mail: mirceafilipsan@gmail.com
Sergiu Ioan Nicolae Mihuț (SINM), SC Integration Support Unit SRL, 35 Baladei Street, 400372 Cluj-Napoca, Romania, e-mail: sergiu.mihut@gmail.com

How to cite this article:
Cetean, H., Cherecheș, A., Filipșan, M., Mihuț, S. I. N. (2027). Integrated UAV-ALS and SLAM-TLS LiDAR for heritage tree inventory and dendrological assessment of a historical park: a case study from Jucu de Sus, Romania. *AES Bioflux, 19*(1), 22-33.